BIOCHEMISTRY
including biophysical chemistry & molecular biology
Article

Biochemistry **2010,** *49,* 10319–10328 10319
DOI: 10.1021/bi100659s

Catalytic Role of the Conformational Change in Succinyl-CoA:3-Oxoacid CoA Transferase on Binding CoA[†,‡]

Marie E. Fraser,* Koto Hayakawa, and William D. Brown

Department of Biological Sciences, University of Calgary, 2500 University Drive NW, Calgary, Alberta T2N 1N4, Canada

Received April 28, 2010; Revised Manuscript Received October 25, 2010

ABSTRACT: Catalysis by succinyl-CoA:3-oxoacid CoA transferase proceeds through a thioester intermediate in which CoA is covalently linked to the enzyme. To determine the conformation of the thioester intermediate, crystals of the pig enzyme were grown in the presence of the substrate acetoacetyl-CoA. X-ray diffraction data show the enzyme in both the free form and covalently bound to CoA via Glu305. In the complex, the protein adopts a conformation in which residues 267−275, 280−287, 357−373, and 398−477 have shifted toward Glu305, closing the enzyme around the thioester. Enzymes provide catalysis by stabilizing the transition state relative to complexes with substrates or products. In this case, the conformational change allows the enzyme to interact with parts of CoA distant from the reactive thiol while the thiol is covalently linked to the enzyme. The enzyme forms stabilizing interactions with both the nucleotide and pantoic acid portions of CoA, while the interactions with the amide groups of the pantetheine portion are poor. The results shed light on how the enzyme uses the binding energy for groups remote from the active center of CoA to destabilize atoms closer to the active center, leading to acceleration of the reaction by the enzyme.

Succinyl-CoA:3-oxoacid CoA transferase (SCOT)[1] catalyzes the transfer of CoA from succinyl-CoA to acetoacetate. Acetoacetate is one of the compounds in ketone bodies. Ketone bodies are produced by the liver and circulated through the bloodstream to extrahepatic tissues, such as the heart and the brain, to be used as a source of energy. In the mitochondria of these tissues, SCOT produces acetoacetyl-CoA, which acetoacetyl-CoA thiolase converts to acetyl-CoA. Acetyl-CoA can then enter the citric acid cycle to provide energy.

Classical biochemical experiments by William Jencks and his research group investigated the catalytic properties of SCOT using enzyme purified from pig heart. They showed that during catalysis the CoA group from succinyl-CoA is transferred to a glutamate residue of SCOT, forming a thioester intermediate (*1*). This glutamate residue was later identified as Glu305 (*2*).[2] Falcone and Boyer had earlier demonstrated that the reaction takes place through an anhydride intermediate (*3*). This means that the transfer of CoA is actually done in two steps: first the succinyl group is transferred to Glu305 to form the anhydride intermediate; then the CoA that has remained associated with the enzyme exchanges with succinate to form the thioester intermediate (*4*). Transfer of CoA to acetoacetate occurs via reversal of the previous steps, with acetoacetate being first linked to Glu305 and then transferred to CoA. This reaction mechanism is thought to be common to all class I CoA transferases and to the class III CoA transferases, which have a different protein fold and an aspartate residue instead of the active site glutamate residue (*5*).

SCOT is an excellent enzyme, accelerating the transfer of CoA by a factor of 10^{16} (*6*), 10^{12} of which comes from interactions with the nonreactive portions of CoA (*7*). These interactions stabilize the transition state relative to either the noncovalent complex with the substrate or the covalently bound thioester intermediate. This mode of stabilization is a feature of enzymes, since it provides acceleration of the rate of the reaction while avoiding inhibition by substrates and products. In only a few cases have the stabilization energies of an enzyme been quantified, and Jencks' group measured these for SCOT using truncated versions of the substrate. The nucleotide portion was found to stabilize the first transition state by −8.9 kcal/mol (*6*), the thioester intermediate by −6.9 kcal/mol (*8*), the second transition state by −8.5 kcal/mol, and the noncovalent complex by only −2.2 kcal/mol (*6*). In contrast, interactions of the pantoic acid portion of CoA with SCOT were found to destabilize the thioester intermediate by 4.8 kcal/mol but stabilize the first transition state by −5.2 kcal/mol, the second transition state by −4.9 kcal/mol, and the noncovalent complex by −1.8 kcal/mol (*6*). The conclusion was that although it was interactions with the nucleotide portion that stabilized the thioester intermediate, the interactions with the pantoic acid portion that destabilized this intermediate led to a large part of the rate acceleration by the enzyme.

[†]This research was supported by a Discovery Grant from the Natural Sciences and Engineering Research Council of Canada (NSERC), Grant MOP-42446 from the Canadian Institutes of Health Research, and equipment grants from NSERC and the Alberta Heritage Foundation for Medical Research (AHFMR). X-ray diffraction data were collected at beamline 8.3.1 of the Advanced Light Source (ALS) at Lawrence Berkeley Laboratory, under an agreement with the Alberta Synchrotron Institute (ASI). The ALS is operated by the Department of Energy and supported by the National Institutes of Health. Beamline 8.3.1 was funded by the National Science Foundation, the University of California, and Henry Wheeler. The ASI synchrotron access program was supported by grants from the Alberta Science and Research Authority and the AHFMR.

[‡]The model and the structure factor amplitudes were deposited to the Protein Data Bank where they were assigned the identifier 3OXO.

*Corresponding author: phone, 1-403-220-6145; fax, 1-403-289-9311; e-mail, frasm@ucalgary.ca.

[1]Abbreviations: SCOT, succinyl-CoA:3-oxoacid CoA transferase; OD_{600nm}, optical density measured at 600 nm; IPTG, isopropyl β-D-thiogalactoside; Tris, tris(hydroxymethyl)aminomethane; PEG, polyethylene glycol; ALS, Advanced Light Source; CNS, Crystallography and NMR System; rmsd, root mean squared deviation.

[2]The numbering of the amino acid residues in this reference included the 39-residue signal sequence. Hence, Glu344 in the reference is actually Glu305.

Published on Web 10/26/2010

A conformational change in SCOT that occurs on forming the thioester intermediate was deduced from studies of the chemical modification of cysteine residues and the inactivation of SCOT (*9*, *10*). However, when a similar class I CoA transferase, Ydif from *Escherichia coli*, was crystallized in both the free form and covalently bound to CoA, the enzyme adopted a similar conformation in both structures (*11*). This conformation was different from that seen in crystal structures of the free form of SCOT (*12*−*14*). We have now crystallized and solved the structure of the SCOT-CoA thioester intermediate. SCOT is a dimeric protein, and the asymmetric unit of the crystals contains four SCOT dimers, two with CoA covalently bound at each of the active sites and two in the free form. These structures, determined under identical conditions, show that SCOT does have a different conformation when CoA is bound. The structure of the SCOT-CoA thioester intermediate allows us to see the interactions with the nucleotide portion that provide stabilization of this intermediate and to understand how the pantoic acid portion provides the destabilization that leads to acceleration of the reaction by the enzyme.

EXPERIMENTAL PROCEDURES

Protein Production. Pig heart SCOT was cloned and overproduced in *E. coli*. To increase the yield and the speed of purification, a carboxy-terminal His_8 tag was added to the protein by ligation of the gene into the pET-42b(+) vector (Novagen). The ligation used a preexisting *Xba*I site upstream of the gene in the pT7-7 vector but required the introduction of an *Xho*I site downstream. Two primers were designed to flank the gene. The forward primer was CGACTCACTATAGGGAGACCACAACGGTTTCCC, and the reverse primer was CCACATTTCAAGT**CTC**GA**G**CTGCTGCATTGGTATCAG. Base changes indicated in bold, in addition to ligation into the vector, changed the carboxy-terminal residues of SCOT from VTT to LEH_8. The polymerase chain reaction (PCR) with Phusion Hot Start High-Fidelity DNA polymerase (Finnzymes) used an initial annealing temperature of 60 °C, which was increased by 0.3 °C per cycle for 20 cycles. The PCR product and pET-42b(+) plasmid DNA were doubly digested with 10 units each of *Xho*I and *Xba*I at 37 °C for 1 h. The digestion products were purified, ligated overnight at 16 °C using T4 DNA ligase, and then transformed into *E. coli* DH5α. Restriction enzyme digests with *Xho*I and *Xba*I checked the ligation, and the gene and flanking regions were subsequently sequenced.

For protein production, *E. coli* BL21(DE3) was transformed with the plasmid. Twenty milliliters of culture grown overnight at 37 °C in Luria−Bertani media was used to inoculate 1 L of Terrific broth. The cells were grown until they reached an OD_{600nm} of 3 approximately 3 h later, at which time protein production was induced with 0.02 mM IPTG, and the cells were grown overnight at 21 °C. The cells were harvested by centrifugation in a Sorvall SLC-6000 rotor at 5×10^3 rpm and 4 °C for 30 min and transferred to 50 mL tubes for storage at −80 °C.

Protein Purification. SCOT was purified using column chromatography with two resins, Ni-NTA agarose (Qiagen) and Ultrogel AcA 44 (Pall). During the purification, the enzyme activity was determined spectrophotometrically by measuring the production of acetoacetyl-CoA in an assay solution containing 0.30 mM succinyl-CoA, 67 mM lithium acetoacetate, 15 mM $MgCl_2$, and 50 mM Tris-HCl, pH 9.1 at 21 °C. The extinction coefficient for acetoacetyl-CoA at 310 nm under these conditions is 7.8×10^3 M^{-1} cm^{-1} (*15*). Total protein concentration was measured using the Bio-Rad protein assay, which is the Bradford assay (*16*). Specific activity and purity, as judged via sodium dodecyl sulfate−polyacrylamide gel electrophoresis, were used to determine which samples to pool during the purification process. The cells containing the protein were thawed and sonicated at 4 °C. The debris was pelleted by centrifugation in a Sorvall SS34 rotor at 1.5×10^4 rpm and 4 °C, and the supernatant was retained. The pellet was resuspended, resonicated, and recentrifuged, again retaining the supernatant. The solution was loaded onto a Ni-NTA agarose column, which was washed with buffer and with buffer containing 50 mM imidazole. SCOT was eluted from the column with buffer containing 250 mM imidazole. After the fractions were concentrated, the sample was loaded onto an AcA 44 column that had been equilibrated with 10 mM Tris-HCl, 10 mM 2-mercaptoethanol, and 1.0 mM benzamidine (pH 8.0) and eluted. The final yield was approximately 10 mg of enzyme/L of initial culture. The specific activity of the purified enzyme was 23.5 μmol min^{-1} mg^{-1}, comparable to that of enzyme produced without the carboxy-terminal purification tag (*14*). After concentration to approximately 20 mg/mL, the protein was quick-frozen in liquid nitrogen (*17*) and stored at −80 °C.

Crystallization. Crystals were grown by vapor diffusion in hanging drops. The protein solution contained 10 mM acetoacetyl-CoA and 5 mg/mL SCOT in 10 mM Tris-HCl (pH 9). A 0.5 μL drop of this solution was mixed with an equal volume of the precipitant solution and then hung over a 1 mL well of the precipitant solution. The crystals grew as thin plates. Even when viewed under the microscope, their quality appeared variable because they grew in layers that had different thicknesses. The piece of crystal used for the data collection was broken from a crystal that had grown with a well solution of 1 mL of 20% PEG-3350 and 100 mM Tris-HCl (pH 8.5) to which 20 μL of 2 M potassium citrate had been added. Its approximate dimensions were $0.12 \times 0.06 \times 0.01$ mm^3. Prior to storage in liquid nitrogen, the crystal was cryoprotected in a solution containing 22.5% PEG-3350, 200 mM potassium citrate, 100 mM Tris-HCl (pH 8.2), and 10% glycerol and vitrified in the cold stream of gaseous nitrogen at 100 K (Oxford Cryostream).

Data Collection and Structure Determination. Crystals were screened, and the diffraction data were collected at beamline 8.3.1 of the Advanced Light Source (ALS) with X-rays of wavelength 1.11588 Å using an ADSC CCD detector. Diffraction data were processed using the Elves scripts (*18*) and programs from the CCP4 package (*19*).

The structure was solved by molecular replacement using the model of a dimer of pig heart SCOT identified in the Protein Data Bank (*20*) as 2NRB, chains A and B (*14*). The program PHASER (*21*) was used in addition to AMoRe (*22*) because PHASER can correct for anisotropic diffraction exhibited by the crystals. Initially, the Crystallography and NMR System (CNS) (*23*) was used for the refinement, but the refinement was completed using REFMAC5 (*24*). The program COOT (*25*) was used to visualize the maps and models and to validate and adjust the models. The quality of the model was also judged using the program MOLPROBITY (*26*).

Several strategies were pursued to obtain the final model. Tight noncrystallographic symmetry restraints greatly improved the model. These restraints were applied to all eight monomers for the majority of residues in the amino-terminal part of the monomer. They were applied separately to each set of four monomers for the carboxy-terminal parts, since it is in the carboxy-terminal part that SCOT binds CoA. The noncrystallographic symmetry

Table 1: Statistics for the Data Set

resolution range (high resolution shell) (Å)	21−2.3 (2.42−2.30)
space group	*P*1
cell dimensions	
a, *b*, *c* (Å)	69.1, 107.1, 134.6
α, *β*, *γ* (deg)	89.6, 80.2, 75.1
R_{merge}[a] (%) (high resolution shell)	8.6 (23.7)
$\langle\langle I\rangle/\sigma(\langle I\rangle)\rangle$[b] (high resolution shell)	5.9 (2.3)
no. of observations $F \geq 0$ (high resolution shell)	283868 (36175)
average redundancy (high resolution shell)	1.9 (1.8)
% completeness (high resolution shell)	91.4 (82.5)
B-factor from Wilson plot (Å^2)	39

[a] $R_{merge} = (\sum\sum|I_i - \langle I\rangle|)/\sum\sum\langle I\rangle$, where I_i is the intensity of an individual measurement of a reflection and $\langle I\rangle$ is the mean value for all equivalent measurements of this reflection. [b] $\langle I\rangle$ is the mean intensity for all reflections; $\langle\sigma(I)\rangle$ is the mean sigma for these reflections.

restraints led to the model being of excellent quality when judged by the validation server, MOLPROBITY (*26*). With the hope of improving the *R*-factors, a correction for the anisotropic diffraction was applied to the diffraction data using the anisotropic diffraction server (*27*). The server recommended a resolution of 2.4 Å in the *b** direction and modified the data accordingly. However, refinement against the corrected data led to worse results than refinement against uncorrected data, likely because the anisotropic diffraction was not severe and could be accommodated better by refinement of the atomic parameters than by the assumptions made by the server in modifying the data. After refinement of the model with individual temperature factors, the TLS Motion Determination server (*28*) was used to break the monomers into groups for rigid body refinement of the TLS parameters. With five identical TLS groups for each monomer that did not bind CoA and five TLS groups for each monomer that bound CoA, the R_{free} and *R*-factors dropped to 26.3% and 24.3%. However, the electron density was worse than when the model was refined with simple isotropic temperature factors. This was likely because tight noncrystallographic symmetry restraints had to be applied to the temperature factors when using TLS groups in the refinement to keep the temperature factors realistic, and the TLS groups chosen were not able to accommodate adequately the differences among the monomers. The final model has tight restraints on the geometry and positions related by noncrystallographic symmetry, with weaker restraints on the temperature factors. Programs from the CCP4 package (*19*) as well as SWISS-PDBVIEWER (*29*), O (*30*), and DYNDOM (*31*) were used to analyze the models.

RESULTS

Crystals of pig heart SCOT grown with acetoacetyl-CoA were of variable quality. Even the best diffracting crystal showed anisotropic diffraction. Statistics from this data set are presented in Table 1. The crystal belongs to the space group *P*1, and from calculations of the Matthews coefficient (*32*, *33*) the crystal was predicted to contain four dimers in the asymmetric unit.

The presence of the four dimers was clear in the molecular replacement solution. Two of the SCOT dimers are in the same conformation as the search model (*14*), while the other two have CoA bound to Glu305 and show the conformational change on binding CoA. The dimers without CoA and the dimers with CoA form alternating layers in the crystal. The solution from which the crystals grew must have contained molecules both with and without CoA. The K_m of SCOT for acetoacetyl-CoA is 0.20 ± 0.04 mM (*7*), while the concentration of acetoacetyl-CoA in the protein solution was 10 mM and the concentration of SCOT, measured as the concentration of monomers or active sites, was approximately 0.1 mM. Even though an excess of acetoacetyl-CoA was used and acetoacetyl-CoA could react with every active site as indicated by the high specific activity of the enzyme, once covalently bound, the CoA-enzyme thioester would be susceptible to hydrolysis. The rate constant for the hydrolysis of the CoA-enzyme thioester is significant, found to be 0.014 (*8*) or 0.10 min^{-1} (*9*) at pH 8.1, depending on the other conditions. Some of the SCOT dimers in solution would be expected to have one monomer without CoA and one with CoA since there is no evidence of alternating site catalytic cooperativity for the formation of the CoA-enzyme thioester (*9*, *34*). The crystallization process is purifying dimers in which the two monomers are identical, layering alternately the dimers without CoA and the dimers with CoA. Although this was significant for the crystallization, it should not be interpreted as demonstrating that the two protomers need to be at the same step in catalysis.

Table 2: Statistics for the Refined Model

no. of data for refinement ($F \geq 0$)	149072
R_{work}[a] (%) (no. of data)	24.5 (141555)
R_{free}[b] (%) (no. of data)	27.3 (7517)
no. of protein atoms	28269
residues in four monomers without CoA	
A	1−247, 259−480
B	1−247, 262−480
C	1−246, 261−480
D	1−246, 260−480
residues in four CoA-binding monomers	
E	1−246, 265−480
F	1−246, 264−480
G	1−245, 267−480
H	1−246, 269−480
no. of atoms in four CoA molecules	192
no. of chloride ions	3
no. of water molecules	440
average *B*-factors for four monomers without CoA, A−D (Å^2)	31, 36, 35, 38
average *B*-factors for four CoA-binding monomers, E−H (Å^2)	43, 45, 45, 55
average *B*-factors for four CoA molecules (Å^2)	52, 55, 47, 68
average *B*-factors for three chloride ions (Å^2)	38
average *B*-factors for water molecules (Å^2)	25
rmsd[c] of bond lengths compared to expected values (Å)	0.006
rmsd of bond angles compared to expected values (deg)	0.9
Ramachandran favored	3608 (98.0%)
Ramachandran outliers	8 (0.2%)

[a] R_{work} is the *R*-factor based on data used in the refinement. *R*-factor = $\sum||F_o| - |F_c||/\sum|F_o|$. [b] R_{free} is the *R*-factor based on data excluded from the refinement (~5%). [c] rmsd is the root mean squared deviation.

The statistics for the refined model are presented in Table 2. The average temperature factors for each of the monomers and for the molecules of CoA are included in this table. It is clear that some of the monomers are better determined than others. Since tight noncrystallographic symmetry restraints were applied in the refinement, the monomers identified as chain A and chain E will be the focus of the discussion.

Electron density for the glutamyl-CoA is shown in Figure 1A. The CoA molecule binds in the funnel formed by the SCOT monomer, extending from Glu305 at the base of the funnel to the surface where the adenosine group is exposed. Figure 1B shows how two CoA molecules bind on opposite faces of a SCOT dimer.

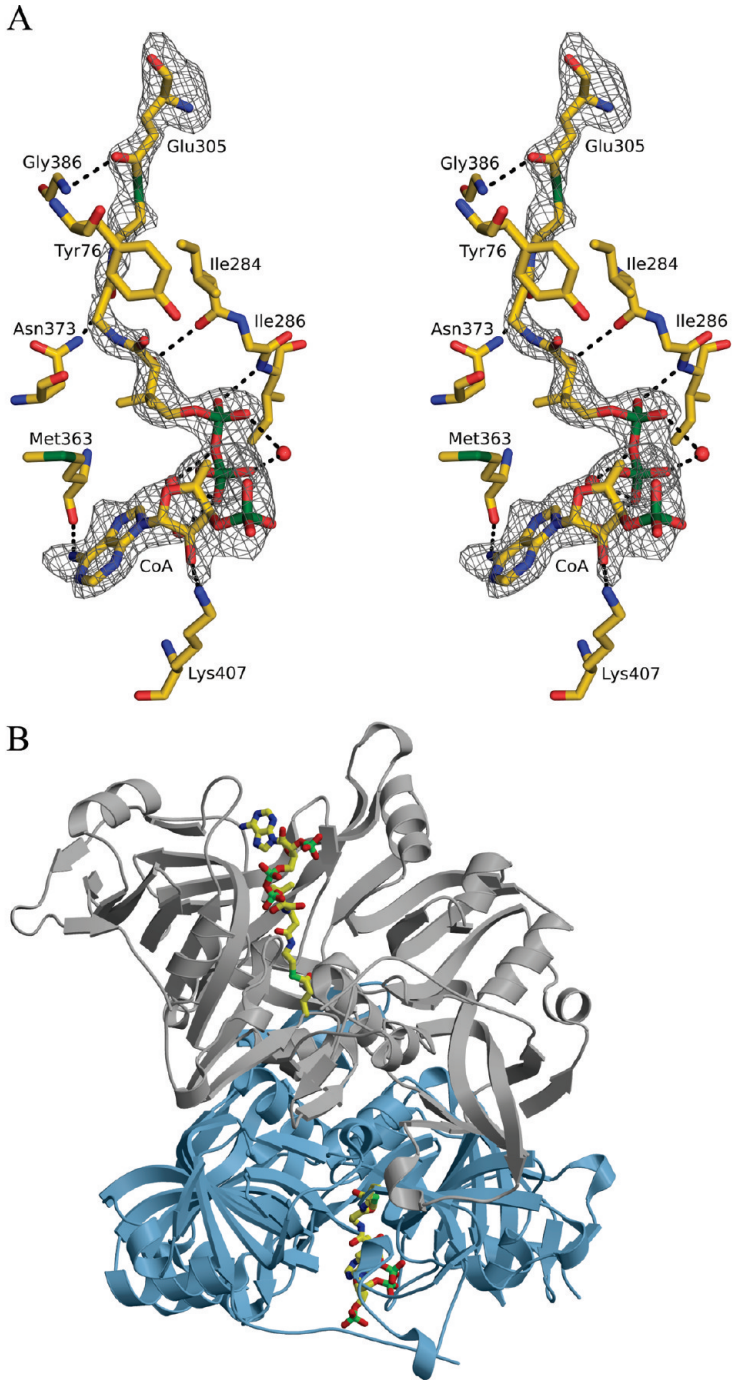

FIGURE 1: (A) Stereoview of the electron density for glutamyl-CoA. The $F_o - F_c$, α_c electron density map, calculated without any of the CoA molecules nor the Glu305 residues to which they are bound, is contoured at 2σ in the region of the CoA molecule bound to chain E. CoA and nearby residues and water molecules, which were included to show hydrogen-bonding interactions (black dashed lines), are drawn as stick models and spheres, colored according to atom type: C, yellow; N, blue; O, red; P and S, green. This figure and Figure 3 were drawn using the program PyMOL (*38*). (B) Ribbon diagram of the SCOT dimer showing the binding sites of CoA. The SCOT monomers are shaded in gray and light blue, the side chains of the Glu305 residues as well as the CoA are drawn as stick models using colors to represent the atom types as in (A). This figure and Figures 2, 4, and 6 were drawn using the programs MOLSCRIPT (*39*) and RASTER3D (*40*).

DISCUSSION

Conformational Change in SCOT. SCOT does change conformation on binding CoA, and the conformational change can be analyzed by comparing the two conformations seen in this crystal structure. Chain A, which does not bind the CoA thioester, and chain E, which does, are superposed in Figure 2. In each of the chains, there is a break in the polypeptide between residue 245 and residue 269, separating each chain into an amino-terminal portion and a carboxy-terminal portion (please see Table 2 for the residue ranges). The conformational change that the enzyme undergoes on binding CoA closes the enzyme, bringing residues from the carboxy terminus, specifically residues 267−275, 280−287, 357−373, and 398−477, toward the rest of the protein as deduced by DYNDOM (*31*). The motion is a rotation of 14° coupled with a translation of 0.5 Å. Although the active site residue, Glu305, with which acetoacetyl-CoA reacts to form the thioester is a residue of the carboxy-terminal portion of the enzyme, it is not part of the domain that moves to

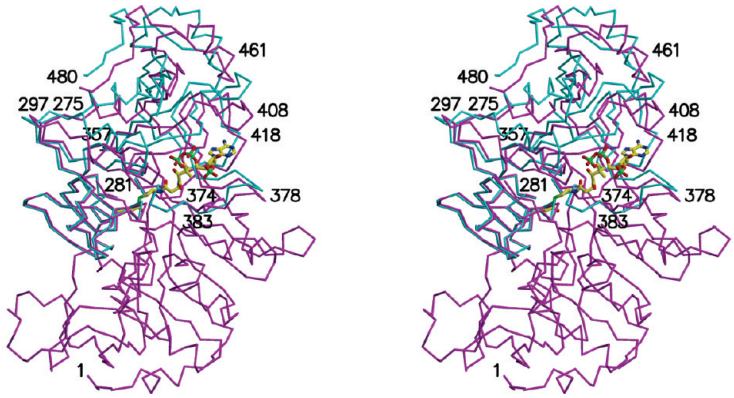

FIGURE 2: Stereoview of the superposition of the Cα traces of free SCOT and the thioester intermediate. The superposition is based on the residues of the amino terminus of SCOT that were restrained by noncrystallographic symmetry to be similar in both chains. The Cα trace of the carboxy-terminal portion of chain A, free SCOT, is drawn in cyan, while the Cα trace of chain E, the thioester intermediate, is drawn in magenta. The side chain of Glu305 and the CoA molecule covalently bound to it are drawn as sticks colored according to the atom types as in Figure 1. The numbers refer to specific residues of the protein.

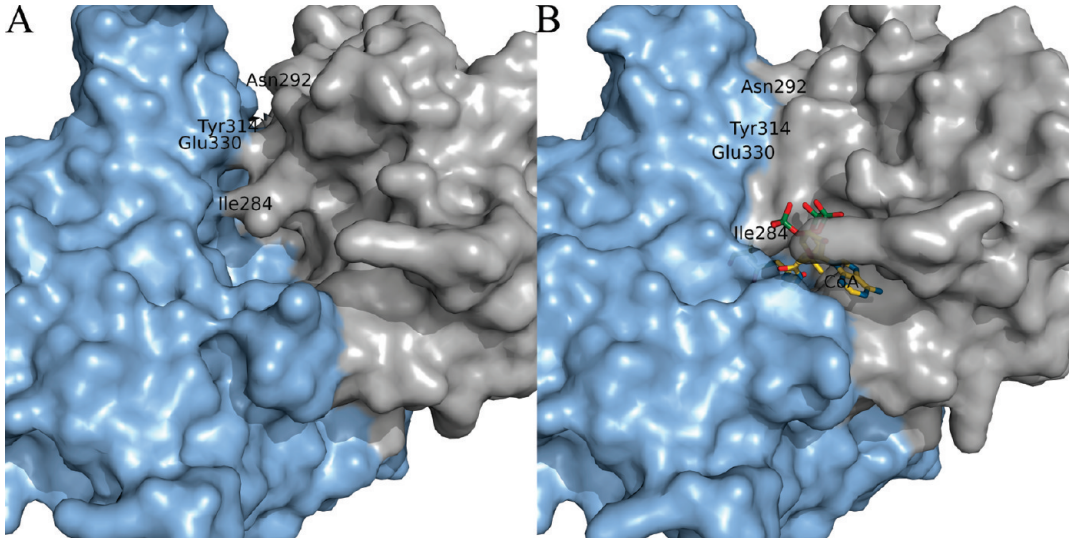

FIGURE 3: Closure of SCOT. Surface diagrams of the binding region of SCOT showing the open conformation of the free enzyme (A) and the closed conformation of the thioester intermediate (B). The surfaces of residues of the amino-terminal portion of the enzyme, residues 302−356 and residues 374−397, are in light blue, while the other residues are in gray. Ile284 and Asn292 on one side of the crevice and Tyr314 and Glu330 on the other side are labeled, as is CoA. CoA is represented as a stick model, colored according to atom type: C, yellow; N, blue; O, red; P and S, green.

close the protein. In general, the motion moves the residues closer to Glu305.

The active site of class I CoA transferases has been described as a funnel with the reactive glutamate residue at the base (*35*). For the structure of SCOT with CoA bound, acetoacetyl-CoA has inserted into the funnel to react with Glu305. The CoA molecule that was transferred to Glu305 fills the funnel, in part because it causes the funnel to seal along one side (Figure 3). This side is where residues 282−287 move toward residues 311−328. Two new hydrogen bonds are found in this region of the closed enzyme, between the hydroxyl of Ser291 and the carbonyl of Gly312 and between the side-chain amide oxygen of Asn292 and the backbone amide nitrogen of Tyr314. The hydrophobic side chains of Ile284 and Leu288 pack near Gly328 and aid in shielding the thioester. On the opposite side of the funnel, the conformational changes in the protein are smaller, but there is also one new hydrogen bond within the protein, where the side chain of Glu84 interacts with the main-chain nitrogen of Val381.

Interactions with CoA in the SCOT-CoA Thioester Intermediate. The conformational change of SCOT allows it to interact with CoA while CoA is covalently bound to the active site glutamate residue. Specific interactions between CoA and other residues of SCOT, including those linked by water molecules, are listed in Table 3. The residues that are from the carboxy terminus and move toward the rest of the protein to enclose CoA in the funnel are underlined in the table. The majority of the interacting residues are in this category. The hydrogen bond between the amino group of the adenine base, N6A, and the carbonyl oxygen of Met363 is notable because it correlates with previous biochemical studies: removal of this amino group reduced k_{cat}/K_M for the reactivation of the enzyme thioester with succinate by a factor of ~40 (*6*). No strong interactions with the 3′-phosphate of CoA are seen in the crystal structure, as expected because similar values of k_{cat}/K_M for the reactivation of the enzyme thioester with succinate were determined for SCOT-3′-dephospho-CoA as for SCOT-CoA (*6*).

CoA could be envisaged binding noncovalently to several of the residues of SCOT in advance of any conformational change. Figure 4 shows the superposition of free SCOT on the SCOT-CoA thioester based on the residues from the carboxy

Table 3: Interactions (Distances ≤3.6 Å) with CoA, Excluding Glu305[a]

portion of CoA		atom	residue	atom	distance (Å)	protein residue interacting with water
nucleotide	adenine	N3A	Ile376	CD1	3.4	
		C2A		CD1	3.4	
		N7A	Met363	CA	3.4	
				CB	3.5	
			water	O	3.4	Lys412
		N6A	Met363	O	2.9	
		C8A	water	O	3.2	Lys412
			water	O	3.5	Lys412, Ala362
	ribose	O2B	Lys407	NZ	2.9	
				CE	3.2	
		O3B	Lys407	NZ	3.4	
		O5B	water	O	3.6	Lys412, Ala362
	5′-phosphates	O1A	water	O	2.4	
		O2A	Glu403	OE1	3.2	
			water	O	2.6	Lys412
			water	O	2.8	Lys412, Ala362
		O3A	water	O	3.5	
			water	O	2.9	Lys412, Ala362
		P1A	water	O	3.2	Lys412, Ala362
			water	O	3.4	
		O4A	Gly285	CA	3.5	
			water	O	3.0	
		O5A	Gly285	CA	3.5	
			Ile286	N	3.0	
			Ile286	CG1	3.5	
pantetheine	pantoic acid	CDP	Asn373	O	3.2	
			Met363	CG	3.4	
		OAP	Ile284	O	3.1	
			Gly361	CA	3.4	
				C	3.4	
				O	3.5	
		CAP	Ile284	O	3.6	
		O9P	Tyr76	OH	3.6	
				CE1	3.5	
		N8P	Asn373	O	3.2	
				ND2	3.4	
		C7P	Gly383	O	3.5	
			Asn373	O	3.2	
		O5P	Asn373	ND2	3.1	
			Ala387	CB	3.6	
		C5P	Met384	O	3.6	
		N4P	Met384	O	3.5	

[a]Residues from the carboxy terminus of SCOT that move toward the rest of the protein to enclose CoA in the funnel are underlined.

terminus that move toward Glu305 in the formation of the thioester intermediate. With the exception of Gly285 and Ile286, the residues that interact with the nucleotide portion of CoA superpose well. This demonstrates that the interactions of these residues with the adenosine 3′-phosphate-5′-diphosphate portion of noncovalently bound CoA could exist simultaneously without any conformational change of the enzyme. These are the interactions with the nucleotide moiety of CoA that "pull the pantetheine moiety into the active site" (*8*).

A conformational change of the enzyme is required for the simultaneous formation of all interactions with the pantoic acid portion of CoA. Figure 4 shows how residues 284−286 shift relative to residues 361−363, which are in similar positions in the two models superposed. The 2 Å shift of residues 284−286 allows the carbonyl oxygen of Ile284 to form a hydrogen bond with the hydroxyl OAP from the pantoic acid portion of CoA. The other interacting residues that shift relative to residues 361−363 are Asn373, which moves ∼1 Å, and Tyr76, which moves almost 4 Å.

Catalysis proceeds through a mixed anhydride, since the acetoacetyl group of acetoacetyl-CoA is transferred to Glu305 prior to the reaction of the free thiol of CoA with the anhydride to form the SCOT-CoA thioester intermediate (*3*). In the open conformation of the enzyme, the nucleotide portion of acetoacetyl-CoA could bind to the enzyme, positioning the substrate so that the sulfur atom is ∼3 Å from the carboxyl carbon of Glu305 (Figure 4). The acetoacetyl group could extend to Glu305, making possible the reaction between the glutamate residue and acetoacetyl-CoA to form the anhydride intermediate. Once the enzyme closed, the free thiol of noncovalently bound CoA would be in position to attack the anhydride, forming the SCOT-CoA thioester intermediate and releasing the acetoacetate.

How Binding to Parts of CoA Remote from the Active Center Aids Catalysis. Experiments measuring the equilibrium constants for the formation of thioesters of SCOT with truncated versions of CoA, starting from the SCOT-CoA thioester, quantified the stability of these thioesters relative to SCOT-CoA

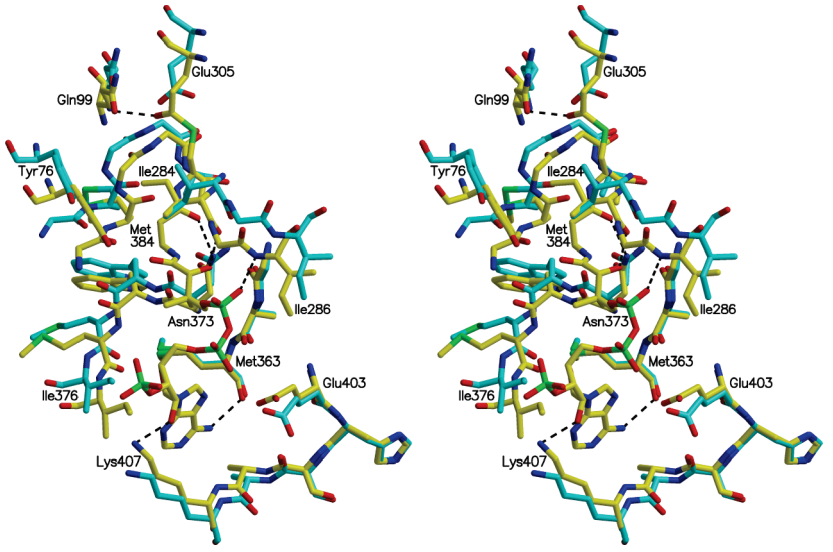

FIGURE 4: Stereoview of the CoA-binding site in the thioester intermediate and in free SCOT. This superposition is based on the residues that move toward Glu305 on binding CoA: 267−275, 280−287, 357−373, and 398−477. The residues are drawn as stick models with the atoms colored according to type: C, yellow for the thioester intermediate and cyan for free SCOT; N, blue; O, red; P and S, green. Select hydrogen-bonding interactions are shown by black dashed lines. The superposition shows that, with the exception of Gly285 and Ile286, all of the interactions with the adenosine 3′-phosphate 5′-diphosphate portion of CoA could be formed prior to any conformational change. In the open conformation of free SCOT, the sulfur atom of the thioester would lie ~3 Å from the carboxyl carbon of Glu305.

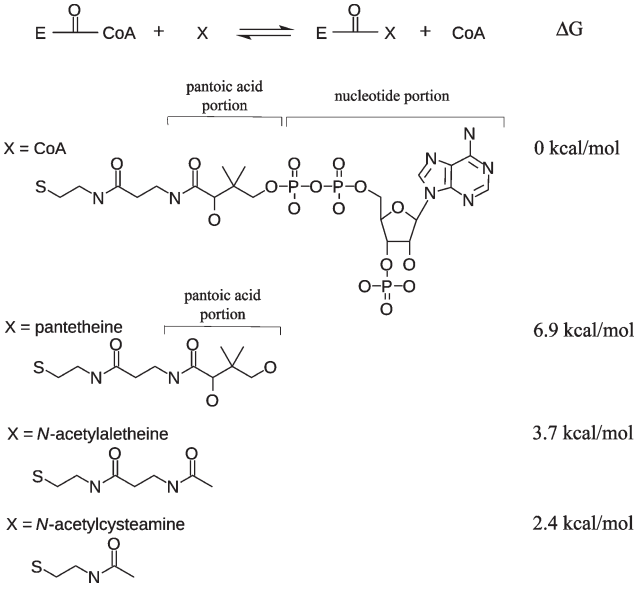

FIGURE 5: Drawing of the chemical reaction used to measure the relative stabilities of the thioesters of SCOT with truncated versions of CoA. Chemical drawings of CoA and of the truncated versions are presented below the reaction, along with the values of ΔG. This figure is adapted from Figure 1 and Table 1 of Whitty et al. (*6*).

(Figure 5). The thioester with CoA was more stable than those with pantetheine, *N*-acetylaletheine, and *N*-acetylcysteamine, by 6.9 (*8*), 3.7, and 2.4 kcal/mol (*6*), respectively. Since pantetheine can be thought of as CoA with the nucleotide portion replaced by hydrogen, or as *N*-acetylcysteamine with both a methylene group and the pantoic acid portion added (Figure 5), the addition of the nucleotide portion stabilizes the SCOT-CoA thioester by 6.9 kcal/mol while the addition of the methylene group and the pantoic acid portion destabilizes the SCOT-pantetheine thioester by 4.5 kcal/mol. This would suggest that the pantoic acid portion destabilizes SCOT-CoA (*6*). However, the destabilization is in comparison with *N*-acetylcysteamine. The atoms of *N*-acetylcysteamine in the SCOT-*N*-acetylcysteamine thioester need not adopt the same conformation that they adopt in SCOT-pantetheine. Without the methylene group and the pantoic acid portion, they could be positioned to form more stable interactions with the protein. The addition of the methylene group and the pantoic acid portion in either the SCOT-pantetheine or the SCOT-CoA thioester may prevent the atoms from the *N*-acetylcysteamine portion from binding in the positions that they adopt in the SCOT-*N*-acetylcysteamine thioester, leading to the higher free energy for the SCOT-pantetheine thioester than for the SCOT-*N*-acetylcysteamine thioester. Hence, the values of the equilibrium constants for the formation of thioesters of SCOT with truncated versions of CoA, starting from the SCOT-CoA thioester, lead to two possible interpretations: either the interactions between the pantoic acid portion of CoA and the active site directly destabilize the SCOT-CoA thioester or they lead to less stable interactions between the *N*-acetylcysteamine
or the *N*-acetylaletheine portion of CoA and the active site. The crystal structure of the SCOT-CoA thioester shows whether the pantoic acid portion provides destabilizing or stabilizing interactions with CoA.

The pantoic acid portion of CoA in the SCOT-CoA thioester appears to have some stabilizing interactions with the enzyme, but its amide group as well as the second amide group of CoA forms poor interactions with residues of the protein. The interactions for the pantoic acid portion that appear to be stabilizing are the van der Waals interactions with its methyl group, CDP, and the hydrogen bond with its hydroxyl, OAP (Table 3). N8P and O9P are part of the amide group of the pantoic acid portion. Although N8P is 3.2 Å from the carbonyl oxygen of Asn373, the orientation of the amide is not correct for hydrogen bonding (Figure 1A). The orientation would be better for a hydrogen bond with Asn373, but ND2 of Asn373, not the oxygen atom, is 3.4 Å from N8P. The orientation of the side chain of Asn373 is defined by the hydrogen bonds donated by ND2 to the carbonyl oxygen of Gly361 and to O5P of CoA. O9P may form a hydrogen bond with the hydroxyl of Tyr76, but this hydrogen bond is only

Table 4: Comparisons between Free and CoA-Bound Structures of SCOT and Structures of *E. coli* Class I CoA Transferase, Ydif, and SCOT Purified from Pig Heart Using a Cutoff of 2 Å To Define Matched Atoms

	comparison with free SCOT (chain A)		comparison with CoA-bound SCOT (chain E)	
CoA transferase (PDB and chain identifier)	rmsd (Å)	no. of Cα atoms	rmsd (Å)	no. of Cα atoms
free SCOT (chain A)	0	469	0.48	357
CoA-bound SCOT (chain E)	0.48	357	0	462
E. coli Ydif (2AHU, chain A)	1.2	160	1.2	189
E. coli Ydif (2AHV, chain A)	1.1	156	1.2	202
SCOT purified from pig heart (3K6M, chain C)	0.41	325	0.38	443
SCOT purified from pig heart (3K6M, chain D)	0.37	441	0.55	341

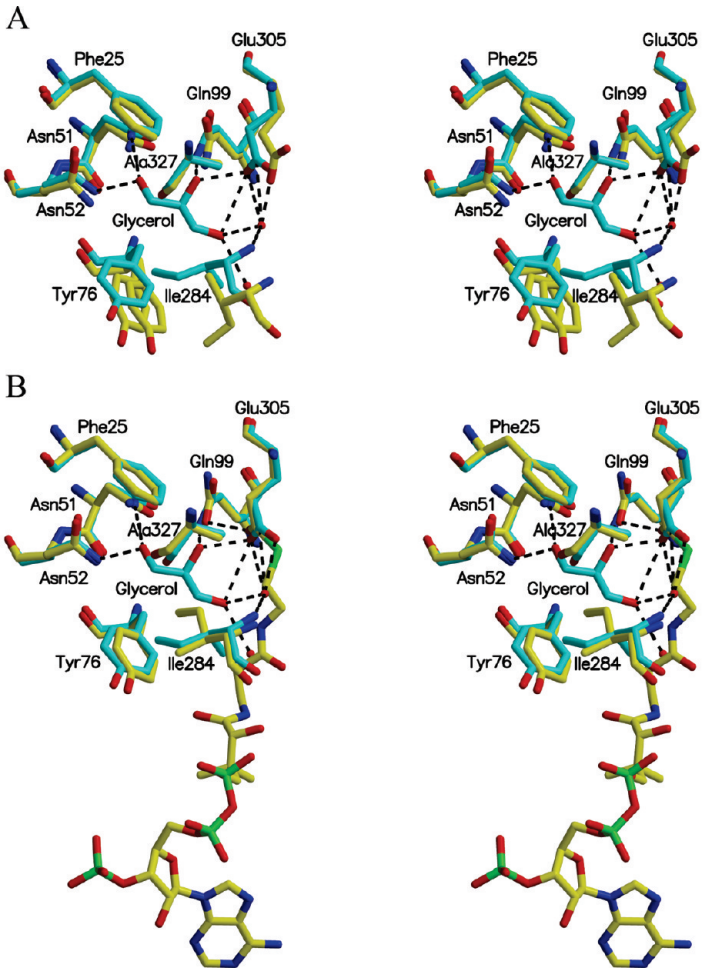

FIGURE 6: Proposed binding site for succinate or acetoacetate. (A) Stereoview of the superposition of glycerol-bound SCOT and free SCOT in the vicinity of the glycerol (*37*). The residues are drawn as stick models with the atoms colored according to type: C, yellow for free SCOT and cyan for glycerol-bound SCOT; N, blue; O, red; P and S, green. Both conformations for Tyr76 in free SCOT are shown. Two water molecules hydrogen-bonded to glycerol are drawn as red spheres. Select hydrogen-bonding interactions are shown by black dashed lines. (B) Stereoview of the superposition of glycerol-bound SCOT (*37*) and the SCOT-CoA thioester in the vicinity of the glycerol. The residues are drawn as stick models with the atoms colored according to type: C, yellow for the SCOT-CoA thioester and cyan for glycerol-bound SCOT; N, blue; O, red; P and S, green.

very weak because the distance between the two atoms is 3.6 Å. In support of this, the mutation of Tyr76 to Phe in mouse SCOT caused a drop in catalytic activity of only 5.6%, demonstrating that this hydrogen bond is not critical for catalysis (*36*). For the second amide group of CoA, O5P accepts a hydrogen bond with a distance of 3.1 Å from ND2 of Asn373, but N4P is 3.5 Å from the carbonyl oxygen of Met 384 and is not oriented for the two to hydrogen bond. If this part of CoA were not restrained by the covalent bond to Glu305 and the noncovalent binding of the pantoic acid portion and the nucleotide portion to the protein, it would undoubtedly reposition to form better interactions with the enzyme. This would be why the SCOT-*N*-acetylcysteamine and *N*-acetylaletheine thioesters are only 2.4 and 3.7 kcal/mol less stable than the SCOT-CoA thioester. The conclusion is that both the nucleotide portion and the pantoic acid portion provide the stabilizing interactions with CoA, and these interactions force the atoms of CoA that lie closer to the reactive thiol to adopt positions in the active site that have higher energy. SCOT uses the binding energy for groups remote from the active center of CoA to destabilize, relative to the configuration that exists in

the transition state for the reaction, atoms closer to the active center, leading to acceleration of the reaction by the enzyme.

Role of the Conformational Change in Binding the Substrate Succinate or Acetoacetate. SCOT has been the prototype for class I CoA transferases, but is it possible that SCOT is the only class I CoA transferase to use a conformational change in the protein on binding CoA to promote catalysis? The structure of SCOT covalently bound to CoA is more similar to the structure of Ydif with or without CoA covalently bound (*11*) than is the structure of free SCOT (Table 4). This suggests that Ydif has only one conformation, the conformation that binds CoA. However, if the energies of the two conformations of a protein are similar, crystal-packing interactions can stabilize one form over the other, selecting which conformation is seen in the crystals. Although the energy difference between the two conformations is not known for Ydif, Jencks' group did measure equilibrium constants for the formation of the SCOT-CoA thioester starting from SCOT and acetoacetyl-CoA or succinyl-CoA (*9*). The equilibrium constant is 9 for the formation of the SCOT-CoA thioester from SCOT and acetoacetyl-CoA, leading to the value of −1.3 kcal/mol for the ΔG of the reaction. The equilibrium constant is 0.24 for the formation from SCOT and succinyl-CoA, leading to the value of +0.84 kcal/mol for ΔG. The small values and their different signs point out that the energy difference between the two conformations of SCOT is small. It is possible that a second conformation also exists for Ydif but that Ydif has not been crystallized in that conformation.

The conformational change seen in SCOT on binding CoA in the SCOT-CoA thioester appears to be important in forming the binding site for the second substrate, succinate or acetoacetate. Recently, the structure of SCOT purified from pig heart was determined in a crystal form where one of the four molecules in the asymmetric unit binds glycerol in the site proposed to bind the substrate succinate or acetoacetate (*37*). Glycerol was included in the purification at the significant concentration of 10% (v/v) or approximately 1.4 M. The SCOT molecule that binds glycerol at the active site has a conformation very similar to that of the SCOT-CoA thioester, while the other three molecules have the conformation of the free form of SCOT (Table 4). The major difference between the two conformations at the proposed binding site for succinate or acetoacetate is in the position of Ile284, which forms van der Waals interactions with glycerol in the complex (Figure 6A). In the structure of the SCOT-CoA thioester (Figure 6B), Ile284 would already have moved into position, preforming the binding site for the substrate succinate or acetoacetate.

ACKNOWLEDGMENT

We thank Jamie Feng and Edward Brownie for production and purification of the protein used for crystallization.

REFERENCES

1. Solomon, F., and Jencks, W. P. (1969) Identification of an enzyme-γ-glutamyl coenzyme A intermediate from coenzyme A transferase. *J. Biol. Chem. 244*, 1079–1081.
2. Rochet, J. C., and Bridger, W. A. (1994) Identification of glutamate 344 as the catalytic residue in the active site of pig heart CoA transferase. *Protein Sci. 3*, 975–981.
3. Falcone, A. B., and Boyer, P. D. (1959) Studies concerning the mechanism of action of acetoacetyl succinic thiophorase by use of O^{18}. *Arch. Biochem. Biophys. 83*, 337–344.
4. Benson, R. W., and Boyer, P. D. (1969) The participation of an enzyme-bound oxygen group in a coenzyme A transferase reaction. *J. Biol. Chem. 244*, 2366–2371.
5. Berthold, C. L., Toyota, C. G., Richards, N. G., and Lindqvist, Y. (2008) Reinvestigation of the catalytic mechanism of formyl-CoA transferase, a class III CoA-transferase. *J. Biol. Chem. 283*, 6519–6529.
6. Whitty, A., Fierke, C. A., and Jencks, W. P. (1995) Role of binding energy with coenzyme A in catalysis by 3-oxoacid coenzyme A transferase. *Biochemistry 34*, 11678–11689.
7. Moore, S. A., and Jencks, W. P. (1982) Formation of active site thiol esters of CoA transferase and the dependence of catalysis on specific binding interactions. *J. Biol. Chem. 257*, 10893–10907.
8. Fierke, C. A., and Jencks, W. P. (1986) Two functional domains of coenzyme A activate catalysis by coenzyme A transferase. *J. Biol. Chem. 261*, 7603–7606.
9. White, H., Solomon, F., and Jencks, W. P. (1976) Utilization of the inactivation rate of coenzyme A trasferase by thiol reagents to determine properties of the enzyme-CoA intermediate. *J. Biol. Chem. 251*, 1700–1707.
10. Kindman, L. A., and Jencks, W. P. (1981) Modification and inactivation of CoA transferase by 2-nitro-5-(thiocyanato)benzoate. *Biochemistry 20*, 5183–5187.
11. Rangarajan, E. S., Li, Y., Ajamian, E., Iannussi, P., Kernaghan, S. D., Fraser, M. E., Cygler, M., and Matte, A. (2005) Crystallographic trapping of the glutamyl-CoA thioester intermediate of family I CoA transferases. *J. Biol. Chem. 280*, 42919–42928.
12. Bateman, K. S., Brownie, E. R., Wolodko, W. T., and Fraser, M. E. (2002) Structure of the mammalian CoA transferase from pig heart. *Biochemistry 41*, 14455–14462.
13. Coros, A. M., Swenson, L., Wolodko, W. T., and Fraser, M. E. (2004) Structure of the CoA transferase from pig heart to 1.7 A resolution. *Acta Crystallogr. D 60*, 1717–1725.
14. Tammam, S. D., Rochet, J. C., and Fraser, M. E. (2007) Identification of the cysteine residue exposed by the conformational change in pig heart succinyl-CoA:3-ketoacid coenzyme A transferase on binding coenzyme A. *Biochemistry 46*, 10852–10863.
15. Howard, J. B., Zieske, L., Clarkson, J., and Rathe, L. (1986) Mechanism-based fragmentation of coenzyme A transferase. Comparison of alpha 2-macroglobulin and coenzyme A transferase thiol ester reactions. *J. Biol. Chem. 261*, 60–65.
16. Bradford, M. M. (1976) A rapid and sensitive method for the quantitation of microgram quantities of protein utilizing the principle of protein-dye binding. *Anal. Biochem. 72*, 248–254.
17. Deng, J., Davies, D. R., Wisedchaisri, G., Wu, M., Hol, W. G., and Mehlin, C. (2004) An improved protocol for rapid freezing of protein samples for long-term storage. *Acta Crystallogr., Sect. D: Biol. Crystallogr. 60*, 203–204.
18. Holton, J., and Alber, T. (2004) Automated protein crystal structure determination using ELVES. *Proc. Natl. Acad. Sci. U.S.A. 101*, 1537–1542.
19. Collaborative Computational Project, N. (1994) The CCP4 suite: Programs for protein crystallography. *Acta Crystallogr. D50*, 760–763.
20. Berman, H. M., Westbrook, J., Feng, Z., Gilliland, G., Bhat, T. N., Weissig, H., Shindyalov, I. N., and Bourne, P. E. (2000) The Protein Data Bank. *Nucleic Acids Res. 28*, 235–242.
21. McCoy, A. J. (2007) Solving structures of protein complexes by molecular replacement with Phaser. *Acta Crystallogr., Sect. D: Biol. Crystallogr. 63*, 32–41.
22. Navaza, J. (1994) AMoRe: an automated package for molecular replacement. *Acta Crystallogr. A50*, 157–163.
23. Brunger, A. T., Adams, P. D., Clore, G. M., Delano, W. L., Gros, P., Grosse-Kunstleve, R. W., Jiang, J.-S., Kuszewski, J., Jilges, N., Pannu, N. S., Read, R. J., Rice, L. M., Simonson, T., and Warren, G. L. (1998) Crystallography and NMR system (CNS): a new software system for macromolecular structure determination. *Acta Crystallogr., Sect. D: Biol. Crystallogr. 54*, 905–921.
24. Murshudov, G. N., Vagin, A. A., and Dodson, E. J. (1997) Refinement of macromolecular structures by the maximum-likelihood method. *Acta Crystallogr., Sect. D: Biol. Crystallogr. 53*, 240–255.
25. Emsley, P., Lohkamp, B., Scott, W. G., and Cowtan, K. (2010) Features and Development of Coot. *Acta Crystallogr., Sect. D: Biol. Crystallogr. 66*, 486–501.
26. Davis, I. W., Leaver-Fay, A., Chen, V. B., Block, J. N., Kapral, G. J., Wang, X., Murray, L. W., Arendall, W. B., III, Snoeyink, J., Richardson, J. S., and Richardson, D. C. (2007) MolProbity: all-atom contacts and structure validation for proteins and nucleic acids. *Nucleic Acids Res. 35*, W375–383.
27. Strong, M., Sawaya, M. R., Wang, S., Phillips, M., Cascio, D., and Eisenberg, D. (2006) Toward the structural genomics of complexes: crystal structure of a PE/PPE protein complex from *Mycobacterium tuberculosis*. *Proc. Natl. Acad. Sci. U.S.A. 103*, 8060–8065.

28. Painter, J., and Merritt, E. A. (2006) TLSMD web server for the generation of multi-group TLS models. *J. Appl. Crystallogr. 39*, 109–111.
29. Guex, N., and Peitsch, M. C. (1997) SWISS-MODEL and the Swiss-PdbViewer: an environment for comparative protein modelling. *Electrophoresis 18*, 2714–2723.
30. Jones, T. A., Zou, J.-Y., Cowan, S. W., and Kjeldgaard, M. (1991) Improved methods for building protein models in electron density maps and the location of errors in these models. *Acta Crystallogr. A47*, 110–119.
31. Hayward, S., and Berendsen, H. J. C. (1998) Systematic analysis of domain motions in proteins from conformational change; new results on citrate synthase and T4 lysozyme. *Proteins: Struct., Funct., Genet. 30*, 144–154.
32. Kantardjieff, K. A., and Rupp, B. (2003) Matthews coefficient probabilities: improved estimates for unit cell contents of proteins, DNA, and protein-nucleic acid complex crystals. *Protein Sci. 12*, 1865–1871.
33. Matthews, B. W. (1968) Solvent content of protein crystals. *J. Mol. Biol. 33*, 491–497.
34. Lloyd, A. J., and Shoolingin-Jordan, P. M. (2001) Dimeric pig heart succinate-coenzyme A transferase uses only one subunit to support catalysis. *Biochemistry 40*, 2455–2467.
35. Jacob, U., Mack, M., Clausen, T., Huber, R., Buckel, W., and Messerschmidt, A. (1997) Glutaconate CoA-transferase from *Acidaminococcus fermentans*: the crystal structure reveals homology with other CoA-transferases. *Structure 5*, 415–426.
36. Wang, Y., Peng, F., Tong, W., Sun, H., Xu, N., and Liu, S. (2010) The nitrated proteome in heart mitochondria of the db/db mouse model: characterization of nitrated tyrosine residues in SCOT, *J. Proteome Res*. (in press).
37. Coker, S.-F., Lloyd, A. J., Mitchell, E., Lewis, G. R., Coker, A. R., and Shoolingin-Jordan, P. M. (2010) The high-resolution structure of pig heart succinyl-CoA:3-oxoacid coenzyme A transferase. *Acta Crystallogr. D66*, 797–805.
38. DeLano, W. L. (2010) The PyMOL Molecular Graphics System, 1.3 ed., Schrödinger, LLC.
39. Kraulis, P. J. (1991) MOLSCRIPT: a program to produce both detailed and schematic plots of protein structures. *J. Appl. Crystallogr. 24*, 946–950.
40. Merritt, E. A., and Bacon, D. J. (1997) Raster3D: photorealistic molecular graphics, in Methods in Enzymology (Carter, C. W., Jr., and Sweet, R. M., Eds.) pp 505−524, Academic Press, New York.